

Got LiZnP? Solution Phase Synthesis of Filled Tetrahedral Semiconductors in the Nanoregime

Received 00th January 20xx,
Accepted 00th January 20xx

Miles A. White,^a Michelle J. Thompson,^a Gordon J. Miller,^{a,b} and Javier Vela^{*a,b}

DOI: 10.1039/x0xx00000x

www.rsc.org/chemcomm

We report the synthesis and characterization of nanocrystalline LiZnP. The reaction proceeds through a zinc metal intermediate followed by rapid incorporation of lithium and phosphorus. We demonstrate flexibility in the selection of Li, Zn, and P precursors, as well as extension of this method to other half-Heusler phases.

Half-Heusler phases are an interesting class of compounds with the general formula XYZ. Their structure can be described as a zinc-blende lattice of Y and Z stuffed with an interpenetrating fcc lattice of X (Figure 1). A special instance of these compounds is when X, Y, and Z are comprised of elements from group I, II, and V, respectively (for instance Li, Zn, and P). These compounds, known as Nowotny-Juza phases,^{1,2,3} have attracted considerable attention due to their potential application in thermoelectric devices,⁴ solar cells,^{5,6} neutron detectors,⁷ and anode materials for Li ion batteries.⁸ The electronic structure of these compounds resembles classic group IV or III-V 8 e⁻ semiconductors because of the presence of the (II-V)⁻ zinc-blende lattice.⁹ Because of this, the band gap of Nowotny-Juza phases can be tuned based on the electronegativity difference of the elements comprising the zinc-blende network.¹⁰

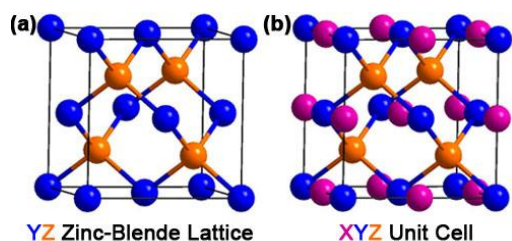
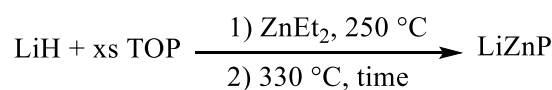


Figure 1. (a) Partial unit cell of half-Heusler XYZ showing the covalent zinc-blende lattice of Y and Z (without X). (b) Full XYZ unit cell with X occupying the octahedral holes in the YZ lattice.

Heavier, n-type 18 e⁻ half-Heusler phases have already shown promise for thermoelectric devices. For instance, Ti doped (Zr,Hf)NiSn displayed a figure of merit (zT) of 1.5 at 700 K.^{11,12} Similarly, a recent computational investigation of Nowotny-Juza phases showed high power conversion efficiencies and large carrier effective masses,⁴ both of which are promising signs of their ability to be used in thermoelectric devices. For example, LiZnSb was suggested as a thermoelectric material with zT ≈ 2 at 600 K.^{13,14} Nowotny-Juza phases have also attracted attention as a buffer layer in CuIn_xGa_{1-x}Se₂ (CIGS) solar cells. This layer should contain a material with a band gap of no less than 2.0 eV and a lattice constant of 5.9 Å.¹⁰ Currently, CdS and other cadmium containing compounds are used to satisfy these criteria. However, an alternative material is desirable due to the toxicity of cadmium. LiZnP has a 2.0 eV band gap, as well as a similar unit cell and lattice parameter compared to CIGS, thus enabling epitaxy between these two materials.

Despite the potential use of LiZnP and other Nowotny-Juza phases in thermoelectric and photovoltaic devices, their synthesis has been limited to the bulk, starting from the constituent elements, through the use of high temperature solid-state reactions.^{7,15,16} A reduction in particle size could lower thermal conductivity which, in turn, could increase thermoelectric efficiency. Additionally, lower temperature and solution phase preparations could be useful in fine-tuning the optical and electronic properties of these materials, decreasing lattice strain, and improving their processability and implementation into flexible devices.^{17,18} Herein, we report the first solution phase synthesis of nanoscale LiZnP and LiCdP.

Nanocrystalline LiZnP was initially synthesized by reacting lithium hydride, diethyl zinc (injected at 250 °C), and an excess of tri-n-octylphosphine (TOP) at 330 °C (Scheme 1).



Scheme 1. Synthesis of nanocrystalline LiZnP.

^aIowa State University, Department of Chemistry, and ^bAmes Laboratory, Ames, Iowa 50011, USA. E-mail: vela@iastate.edu

Electronic Supplementary Information (ESI) available: Additional powder XRD, SAED, XPS, TGA/DSC, and TEM images can be found in the supplementary information document. See DOI: 10.1039/x0xx00000x

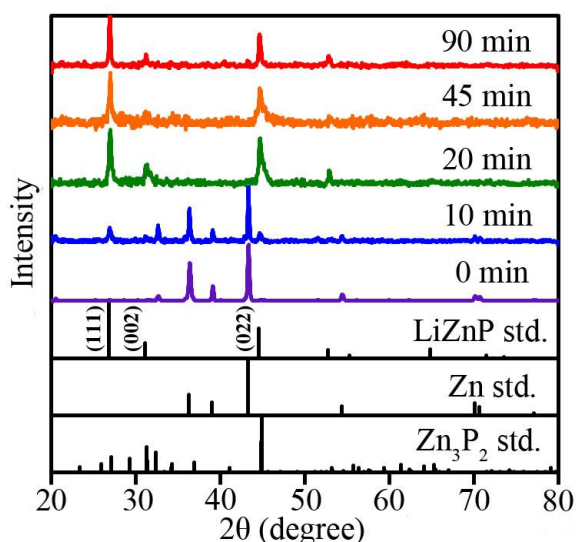


Figure 2. Powder XRD of solids isolated after reacting LiH, Et₂Zn and TOP at different time and 330 °C. Std. patterns are in black.

TOP was chosen as a P source due to its ability to simultaneously act as both solvent and surface passivating ligand. The reaction was monitored by precipitating the solid products and analyzing them by powder X-ray diffraction (XRD) (Figure 2). Our data clearly show that metallic zinc forms immediately upon injection of diethyl zinc into the reaction mixture. This behavior is reminiscent of that reported during the colloidal synthesis of other metal phosphide nanoparticles that utilize TOP as the P source.^{19,20,21,22,23,24,25} LiZnP begins to be observable after 10 min of reaction at 330 °C, and becomes the only crystalline phase observable by XRD within 20 min. Longer reaction times do not appear to have any detrimental effect on crystallinity or particle size (estimated from Scherrer equation). To test whether the reaction truly progresses through a Zn metal intermediate, Zn metal nanoparticles were synthesized *ex situ* and subsequently used as the injected Zn source (*in lieu* of ZnEt₂). As before, this reaction yielded a majority of nanocrystalline LiZnP (see Figure S1).

Using a transmission electron microscope (TEM), energy-dispersive X-ray spectroscopy (EDX) (see Figures S2 and S3) was employed to further characterize the LiZnP particles. While this technique is unable to detect the light (low Z) Li element, EDX allows gathering critical information about the relative Zn and P content. Representative data taken from several sample areas showed 36.3 ± 0.7 atom% Zn and 63.7 ± 0.4 atom% P. We attribute the deviation from the anticipated 1:1 Zn to P ratio to the presence of excess ligand (TOP) in the sample. This hypothesis is supported by TEM and XPS measurements, which show some amorphous material surrounding the nanocrystals (see Figure S2 and S3).

Distinct powder rings without outlier reflections in the selected area electron diffraction (SAED) show the high level of crystallinity possessed by these particles as well as the absence of other identifiable crystalline phases (see Figure S2). The observed reflections correspond well to the lattice *d*-spacings expected for LiZnP. The most intense reflection (111) is located

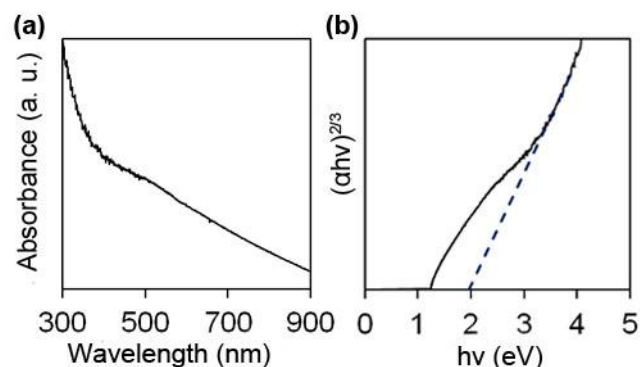


Figure 3. (a) UV-Vis absorbance spectra for LiZnP and (b) Tauc plot displaying its direct forbidden gap of 2.0 eV.

very near the beam stop and is difficult to discern. Instead, the second most intense reflection (022) is the first easily observed ring. As such, this ring is the most prominent in the SAED. All other observed reflections agree with LiZnP *d*-spacings.

The electronic and optical properties of LiZnP nanoparticles are important for their potential integration into energy conversion devices. The optical absorption spectrum of LiZnP is consistent with the direct forbidden band gap reported for this material.^{15,26,27} The magnitude of this gap was found to be 2.0 eV using a Tauc plot (Figure 3). A lack of sharp absorption features suggests the LiZnP particles are not quantum confined. This is understandable based on the large effective carrier masses of Nowotny-Juza phases,⁴ which are nonetheless ideal for the development of more efficient thermoelectric materials.

We have sought to probe the synthetic flexibility of our reaction by investigating the use of alternative precursors. We specifically looked to increase the homogeneity of the reaction through the use of soluble organolithium reagents, as well as to develop less reactive zinc reagents. Various organolithium reagents are widely accessible, and some are known to undergo reductive elimination at elevated temperatures to yield LiH.²⁸ Repeating the parent reaction with *n*-butyllithium (*n*-BuLi), lithium diisopropylamide (LDA), or phenyllithium (PhLi) instead of LiH yielded phase pure LiZnP (see Figure S5). Critically, the ability to better control the quantity of lithium added using one of these two soluble reagents allowed us to control the particle size by simply fine-tuning the reaction stoichiometry. Altering the Li to Zn from 1:1 to 5:1 changed the LiZnP particle size from 10 nm to 25 nm (estimated by the Scherrer equation, see Figure S6).

In our search for non-pyrophoric, safer alternatives to Et₂Zn, we found that either zinc stearate (ZnSt₂) and zinc chloride (ZnCl₂) can be used to successfully generate LiZnP (see Figure S7). The use of a zinc carboxylate, in particular, is not only greener, but also potentially beneficial for size control. In the case of Zn₃P₂, it has been demonstrated that passivation with a carboxylate ligand results in much smaller particle size than that observed with TOP.²⁹ Similarly, we found that other phosphines such as triphenylphosphine (Ph₃P, m.p. = 80.5 °C) can also be successfully used as a solvent and phosphorous

source instead of TOP, although this required longer reaction times to form LiZnP (6 h, PPh₃ vs. 20 min, TOP).

Finally, based on our ability to synthesize LiZnP nanocrystals with a variety of reagents and conditions, we sought to generalize the scope of our approach to the synthesis of other Nowotny-Juza phases. To test this hypothesis, we replaced dimethyl cadmium for diethyl zinc in the parent reaction in an attempt to synthesize LiCdP. Powder XRD reveals the formation of majority phase LiCdP, accompanied by a Cd₃P₂ impurity phase (see Figure S8). While some optimization is needed in order to remove excess ligand (from LiZnP) or impurity phases (from LiCdP), the ability to generate nanocrystals of both Nowotny-Juza phases through a simple, low temperature solution phase method with a variety of reagents is encouraging. More generally, a broader survey of the solution-phase synthesis of other nanocrystalline Nowotny-Juza compounds is warranted, although this is beyond the scope of this communication.

In conclusion, nanocrystalline LiZnP and LiCdP were prepared at low temperature using solution phase synthesis. Our general approach relies on the use of a neat, high boiling phosphine such as TOP or PPh₃ as both phosphorus source and solvent, and proceeds through the *in situ* generation of an intermediate metallic phase (for example, Zn). Powder XRD and TEM data showcase the high crystallinity as well as the relative thermal stability of LiZnP. Further, the optical properties match those of the bulk. Because of its synthetic flexibility and generality, this synthetic approach has the potential to be useful in the preparation of other Nowotny-Juza phases. Future experiments will explore the effects of stoichiometry and precursor reactivity on the composition, size and shape control of these and other related nano phases.^{30,31}

J. Vela thanks the US National Science Foundation for a CAREER grant from the Division of Chemistry, Macromolecular, Supramolecular and Nanochemistry program (1253058).

Notes and references

- ¹ Zakutayev, A.; Zhang, X.; Nagaraja, A.; Yu, L.; Lany, S.; Mason, T. O.; Ginley, D. S.; Zunger, A. *J. Am. Chem. Soc.* 2013, **135**, 10048.
- ² Nowotny, H.; Bachmayer, K. *Monatsh. Chem.* 1950, **81**, 488.
- ³ Juza, R.; Hund, F. Z. *Anorg. Chem.* 1948, **257**, 1.
- ⁴ Yadav, M. K.; Sanyal, B. *J. Alloy. Compd.* 2015, **622**, 388.
- ⁵ Casper, F.; Graf, T.; Chadov, S.; Balke, B.; Felser, C. *Semicond. Sci. Technol.* 2012, **27**, 063001.

- ⁶ Kieven, D.; Grimm, A.; Beleanu, A.; Blum, C. G. F.; Schmidt, J.; Rissom, T.; Lauermaun, I.; Gruhn, T.; Felser, C.; Klenk, R. *Thin Solid Films* 2011, **519**, 1866.
- ⁷ Montag, B. W.; Reichenberger, M. A.; Arpin, K. R.; Sunder, M.; Nelson, K. A.; Ugorowski, P. B.; McGregor, D. S. *J. Cryst. Growth* 2015, **412**, 103.
- ⁸ Beleanu, A.; Mondeshki, M.; Juan, Q.; Casper, F.; Felser, C.; Porcher, F. *J. Phys. D: Appl. Phys.* 2011, **44**, 475302.
- ⁹ Kuriyama, K.; Takahashi, Y.; Tomizawa, K. *Phys. Rev. B* 1993, **47**, 13861.
- ¹⁰ Kieven, D.; Klenk, R.; Naghavi, S.; Felser, C.; Gruhn, T. *Phys. Rev. B* 2010, **81**, 075208.
- ¹¹ Sakurada, S.; Shutoh, N. *Appl. Phys. Lett.* 2005, **86**, 082105.
- ¹² Downie, R. A.; MacLaren, D. A.; Smith, R. I.; Bos, J. W. G. *Chem. Commun.* 2013, **49**, 4184.
- ¹³ Madsen, G. K. H. *J. Am. Chem. Soc.* 2006, **128**, 12140.
- ¹⁴ Toberer, E. S.; May, A. F.; Scanlon, C. J.; Snyder, G. J. *J. Appl. Phys.* 2009, **105**, 063701.
- ¹⁵ Kuriyama, K.; Katoh, T.; Mineo, N. *J. Cryst. Growth* 1991, **108**, 37.
- ¹⁶ Bacewicz, R.; Ciszek, T. F. *Appl. Phys. Lett.* 1988, **52**, 1150.
- ¹⁷ Lubner, E. J.; Mobarok, M. H.; Buriak, J. M. *ACS Nano* 2013, **7**, 8136.
- ¹⁸ Bux, S. K.; Fleurial, J.-P.; Kaner, R. B. *Chem. Commun.* 2010, **46**, 8311.
- ¹⁹ Mobarok, M. H.; Lubner, E. J.; Bernard, G. M.; Peng, L.; Wasylshen, R. E.; Buriak, J. M. *Chem. Mater.* 2014, **26**, 1925.
- ²⁰ Henkes, A. E.; Vasquez, Y.; Schaak, R. E. *J. Am. Chem. Soc.* 2007, **129**, 1896.
- ²¹ Henkes, A. E.; Schaak, R. E. *Chem. Mater.* 2007, **19**, 4234.
- ²² Carenco, S.; Portehault, D.; Boissière, C.; Mézailles, N.; Sanchez, C. *Chem. Rev.* 2013, **113**, 7981.
- ²³ Chiang, R.-K.; Chiang, R.-T. *Inorg. Chem.* 2007, **46**, 369.
- ²⁴ Muthuswamy, E.; Kharel, P. R.; Lawes, G.; Brock, S. L. *ACS Nano* 2009, **3**, 2383.
- ²⁵ Brock, S. L.; Senevirathne, K. *J. Solid State Chem.* 2008, **181**, 1552.
- ²⁶ Kuriyama, K.; Katoh, T. *Phys. Rev. B* 1988, **37**, 7140.
- ²⁷ Wood, D. M.; Zunger, A.; Groot, R. de. *Phys. Rev. B* 1985, **31**, 2570.
- ²⁸ Finnegan, R. A.; Kutta, H. W. *J. Org. Chem.* 1965, **30**, 4138.
- ²⁹ Glassy, B. A.; Cossairt, B. M. *Chem. Commun.* 2015, **51**, 5283.
- ³⁰ Ruberu, T. P. A.; Albright, H. R.; Callis, B.; Ward, B.; Cisneros, J.; Fan, H.-J.; Vela, J. *ACS Nano* 2012, **6**, 5348.
- ³¹ Andaraarachchi, H. P.; Thompson, M. J.; White, M. A.; Fan, H.-J.; Vela, J. *Chem. Mater.* 2015, **27**, 8021.